INTERNATIONAL JOURNAL OF OPTIMIZATION IN CIVIL ENGINEERING
Int. J. Optim. Civil Eng., 2016; 6(2):303-317

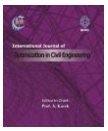

ISOGEOMETRIC TOPOLOGY OPTIMIZATION OF STRUCTURES CONSIDERING WEIGHT MINIMIZATION AND LOCAL STRESS CONSTRAINTS

H.S. Kazemi, S.M. Tavakkoli[*, †] and R. Naderi
Department of Civil Engineering, Shahrood University, Shahrood, Iran

ABSTRACT

The Isogeometric Analysis (IA) is utilized for structural topology optimization considering minimization of weight and local stress constraints. For this purpose, material density of the structure is assumed as a continuous function throughout the design domain and approximated using the Non-Uniform Rational B-Spline (NURBS) basis functions. Control points of the density surface are considered as design variables of the optimization problem that can change the topology during the optimization process. For initial design, weight and stresses of the structure are obtained based on full material density over the design domain. The Method of Moving Asymptotes (MMA) is employed for optimization algorithm. Derivatives of the objective function and constraints with respect to the design variables are determined through a direct sensitivity analysis. In order to avoid singularity a relaxation technique is used for calculating stress constraints. A few examples are presented to demonstrate the performance of the method. It is shown that using the IA method and an appropriate stress relaxation technique can lead to reasonable optimum layouts.

Keywords: topology optimization; isogeometric analysis; local stress constraints; stress relaxation technique; MMA.

Received: 13 October 2015; Accepted: 19 December 2015

1. INTRODUCTION

In general, structural optimization aims to find the best structure so that applied loads are sustained and transferred to specified supports in an appropriate way. To reach the point, there are three types of structural optimization named topology, shape and size

[*]Corresponding author: Department of Civil Engineering, Shahrood University, Shahrood, Iran
[†]E-mail address: mtavakkoli@shahroodut.ac.ir (S. M. Tavakkoli)

optimizations. In topology optimization approach, optimum layout that means number, location and size of the holes in a structure, is sought. Subsequently, shape of boundaries of the structure and size or thickness of members are optimized through shape and size optimization methods, respectively [1,2].

During the last two decades topology optimization methods have been improved by many researchers. In pioneering procedures on structural topology optimization, introduced by BendsØe and Kikuchi, the homogenization theory is used to parameterize the problem [3]. For the sake of simplicity, the Solid Isotropic Materials with Penalization (SIMP) approach was later on developed where the need for homogenization process is eliminated [4].

To solve the topology optimization problem several methods such as optimality criteria (OC) methods [4,5], the approximation methods [6-8], CONLIN [9] and the Method of Moving Asymptotes (MMA) [10], even more heuristic methods such as genetic algorithm [11-13] and Ant colony [14] are employed. Also, less mathematically rigorous methods such as the evolutionary structural optimization method (ESO) can be named [15]. Moreover, several different approaches are devised that use the Level Set methods (LS) [16-19]. As an optimization engine the MMA method is used here which has been proven to be amongst the most effective to solve the topology optimization problems.

In this research, the optimization problem aims to minimize weight of a structure subject to stress constraints. There are several researches in literature carried out to improve the performance of the minimum weight problem including accuracy and computational costs [23-31]. In these methods, relative density of finite elements of discretized domain are considered as design variables and stress constraints are calculated for intermediate node of each element, called local stress constraints [20-22]. In addition, in order to avoid singularity, due to increasing stress in less material areas, the stress relaxation technique is usually employed [32-36].

The IA method has been developed by Hughes and his co-workers in recent years [37-41]. This method is a logical extension and generalization of the classical finite element method and has many features in common with it. However, it is more geometrically based and takes inspiration from Computer Aided Geometry Design (CAGD). A primary goal of IA is to be geometrically precise no matter how coarse the discretization beside simplification of mesh refinement by eliminating the need for communication with the CAD geometry once the initial model is constructed. The main idea of the method is to use the same basis functions which are employed for geometry description for approximation and interpolation of the unknown field variables as well. Due to some interesting properties of B-splines and NURBS, they are perfect candidates for this purpose.

The IA method has been utilized for topology optimization of structures instead of the FE approach; where the NURBS basis functions have also been used for approximating the material density function [42,43]. The method presented in this article falls within the category of nodal based methods which uses control points instead of nodal points and employs the IA approach. The material distribution function is approximated over the whole domain and is restricted to be within zero (for empty areas or voids) and one (for solid areas) interval. Also, similar to the SIMP method a penalty exponent is implemented to suppress formation of undesirable porous media inside the optimal layout [42,43].

In Section 2, the IA method for plane stress problems is briefly explained. Section 3 is devoted to the concise definition of the topology optimization problem. In Section 4,

sensitivity analysis is carried out using the direct analytical method. Three examples are presented in section 5 to demonstrate the performance of the method. Finally, the results are discussed in the last section.

2. ISOGEOMETRIC ANALYSIS

The procedure of the IA for elasticity problems is comprised of the following steps. First, the geometry of the domain of interest is constructed by using the NURBS technology. Depending on the complexity of the geometry and topology of the problem, multiple NURBS patches can be used in this stage. These patches may be thought of as kind of macro elements in the finite element method and can be assembled in the same fashion [37]. In the next step, borrowing the ideas from isoparametric finite elements, the geometry as well as the displacement components are approximated by making use of the NURBS basis functions. Then, following a standard procedure like the weighted residuals or the variational methods, or similarly using the principle of virtual work, the approximated quantities are substituted into the obtained relations. This will result in a system of linear equations to be solved. One should note that following this procedure the control variables are evaluated and to obtain the displacements at certain points a kind of post processing is required. A brief introduction to the construction of NURBS surfaces followed by derivation of IA formulation for plane elasticity problems are the subjects of the next two subsections.

2.1 Surface and volume definition by NURBS

A NURBS surface is parametrically constructed as [44]:

$$S(\xi,\eta)=\frac{\sum_{i=1}^{n}\sum_{j=1}^{m}N_{i,p}(\xi)N_{j,q}(\eta)\omega_{i,j}P_{i,j}}{\sum_{i=1}^{n}\sum_{j=1}^{m}N_{i,p}(\xi)N_{j,q}(\eta)\omega_{i,j}} \tag{1}$$

where $P_{i,j}$ are ($n\times m$) control points, $\omega_{i,j}$ are the associated weights and $N_{i,p}(\xi)$ and $N_{j,q}(\eta)$ are the normalized B-splines basis functions of degree p and q respectively. The i-th B-spline basis function of degree p, denoted by $N_{i,p}(\xi)$, is defined recursively as:

$$N_{i,0}(\xi)=\begin{cases}1 & \text{if } \xi_i\le\xi\le\xi_{i+1}\\ 0 & \text{otherwise}\end{cases}\quad N_{i,p}(\xi)=\frac{\xi-\xi_i}{\xi_{i+p}-\xi_i}N_{i,p-1}(\xi)+\frac{\xi_{i+p+1}-\xi}{\xi_{i+p+1}-\xi_{i+1}}N_{i+1,p-1}(\xi) \tag{2}$$

where $\boldsymbol{\xi}=\{\xi_0,\ \xi_1,\ldots,\xi_r\}$ is the knot vector and ξ_i are a non-decreasing sequence of real numbers, which are called knots. The knot vector $\boldsymbol{\eta}=\{\eta_0,\ \eta_1,\ldots,\eta_s\}$ is employed to define the $N_{j,q}(\eta)$ basis functions for other direction. The interval $[\xi_0,\xi_r]\times[\eta_0,\eta_s]$ forms a patch [37]. A knot vector, for instance in ξ direction, is called open if the first and last knots have a multiplicity of p+1. In this case, the number of knots is equal to $r=n+p$. Also, the interval $[\xi_i,\xi_{i+1})$ is called a knot span where at most p+1 of the basis functions $N_{i,p}(\xi)$ are non-zero

which are $N_{i\text{-}p,p}(\xi)$, …, $N_{i,p}(\xi)$. For some details Reference [44] can be consulted.

2.2 Numerical formulation for plane elasticity problems

In the IA method, the domain of problem might be divided into subdomains or patches so that B-spline or NURBS parametric space is local to these patches. A patch is like an element in the finite element method and the approximation of unknown function can be written over a patch. Therefore, the global coefficient matrix, which is similar to the stiffness matrix in elasticity problems, can be constructed by employing the conventional assembling which is used in the finite element method.

By using the NURBS basis functions for a patch p, the approximated displacement functions $\mathbf{u}^p=[u,v]$ can be written as:

$$\mathbf{u}^p(\xi,\eta)=\sum_{i=1}^{n}\sum_{j=1}^{m}R_{i,j}(\xi,\eta)\mathbf{u}^p{}_{i,j} \tag{3}$$

where $R_{i,j}(\xi,\eta)$ is the rational term in Equation (1). It should be noted that the geometry is also approximated by B-spline basis functions as:

$$\mathbf{s}^p(\xi,\eta)=\sum_{i=1}^{n}\sum_{j=1}^{m}R_{i,j}(\xi,\eta)\mathbf{s}^p{}_{i,j} \tag{4}$$

By using the local support property of NURBS basis functions, the above relation can be summarized as it follows in any given $(\xi,\eta)\in[\xi_i,\xi_{i+1})\times[\eta_j,\eta_{j+1})$.

$$\mathbf{u}^p(\xi,\eta)=(u^p(\xi,\eta),v^p(\xi,\eta))=\sum_{k=i-p}^{i}\sum_{l=j-q}^{j}R_{k,l}(\xi,\eta)U^p{}_{k,l}=\mathbf{RU} \tag{5}$$

$$\mathbf{s}^p(\xi,\eta)=(x^p(\xi,\eta),y^p(\xi,\eta))=\sum_{k=i-p}^{i}\sum_{l=j-q}^{j}R_{k,l}(\xi,\eta)P^p{}_{k,l}=\mathbf{RP} \tag{6}$$

The strain-displacement matrix **B** can be constructed from the following fundamental equations:

$$\boldsymbol{\varepsilon}=\mathbf{Du}\rightarrow\boldsymbol{\varepsilon}=\mathbf{BU} \tag{7}$$

where **D** is the differential operation matrix. Following a standard approach for the derivation of the finite elements formulation, the matrix of coefficients can easily be obtained. For example, by implementing the virtual displacement method with existence of body forces **b** and traction forces **t** we can write:

$$\int_{V^p}\delta\boldsymbol{\varepsilon}^T\boldsymbol{\sigma}dV-\int_{V^p}\delta\mathbf{u}^T\mathbf{b}dV-\int_{\Gamma^p}\delta\mathbf{u}^T\mathbf{t}d\Gamma=0 \tag{8}$$

where V^p and Γ^p are the volume and the boundary of patch p.

Now, by substituting $\delta\boldsymbol{\varepsilon}=\mathbf{B}\delta\mathbf{U}$ from Equation (7) and the constitutive equation $\boldsymbol{\sigma}=\mathbf{C}\boldsymbol{\varepsilon}$, in Equation (8) and by dropping the non-zero coefficient of $\delta\mathbf{U}^T$, the matrix of coefficients can be obtained as:

$$\mathbf{K}^p = \int_{V^p} \mathbf{B}^T \mathbf{C}\mathbf{B} dV \tag{9}$$

3. TOPOLOGY OPTIMIZATION PROBLEM

In this paper, the topology optimization problem is how to distribute the minimum material to form a structure in which the stresses are less than a certain allowable stress. Spatial material distribution can be described as a density function $\phi(\mathbf{x})$ for every point x of the design domain [2], which is considered between zero and one for empty and solid areas, respectively. The density function can also be approximated using the NURBS basis functions as follows:

$$\phi^p(\xi,\eta) = \sum_{i=1}^{n}\sum_{j=1}^{m} R_{i,j}(\xi,\eta)\Phi^p{}_{i,j} \tag{10}$$

where $\phi(\xi,\eta)$ is the density function and $\Phi^p{}_{i,j}$ are control points of the density function created by NURBS in patch p that can be assumed as design variables of the optimization problem. It is noted that the same basis functions are used for approximating geometry, displacements and the density function. Inspired by the SIMP method, in order to prevent the porous area, the density function is penalized for evaluating the artificial elasticity matrix. Therefore:

$$\mathbf{C}_{ijkl} = \phi^{\mu}(\xi,\eta)\mathbf{C}^0_{ijkl} \tag{11}$$

where $\mathbf{C}$ is the elasticity matrix, μ is penalization exponent that is usually considered more than 3 [45].

As it mentioned before, the optimization problem aims to minimize the total weight of the structure (W) that can be obtained as below:

$$W = \int_{\Omega} \phi(\xi,\eta) d\Omega \tag{12}$$

Also, the von Mises stresses is employed as stress constraints which is defined in 2D problems as follows:

$$\sigma_{von} = \sqrt{0.5\times((\sigma_x-\sigma_y)^2+\sigma_x^2+\sigma_y^2+6\tau_{xy}^2)} = \sqrt{\sigma_x^2+\sigma_y^2-\sigma_x\sigma_y+3\tau_{xy}^2} \tag{13}$$

where σ_x and σ_y are the normal stresses and τ_{xy} is the shear stress.

It is worth noting that generally when material is removed in some areas of the domain during the optimization process, the stress constraints might be violated and prevents removing all materials from the areas. Sved and Ginos in 1968 found that stress constraints are not satisfied as the bar area goes to zero in a truss optimization problem and the bar can thus not be removed (known as singularity) [32]. This singularity can also emerge in two and three dimensional continuum problems where non-disappearing stresses remain as the design variables go towards zero. In other words, a region with low design variable values can still have strain which give rise to stress with a nonzero and sometimes remarkably high value while it actually should be zero as it represents a hole. The singularity problem has been discussed in several research papers [32-34]. A remedy to avoid the problem is to use an ε-relaxation approach as suggested by Cheng and Guo in 1997 [35]. According to this approach, main stress constraints are replaced with relaxed stress constraints so that for any $\varepsilon>0$, the ε-relaxed problem is characterized by a design space that is not any longer degenerate and optimization problem is converged better to a solution [2].

Eventually, the discretized optimization problem considering stress relaxation approach can be written as below [46],

$$\begin{aligned} &\min_{\Phi_{i,j}} \quad W(\Phi_{i,j}) \\ &subject\ \ to: \quad \mathbf{Ku}=\mathbf{f} \\ &\sigma_{von} \le (1-\varepsilon+\frac{\varepsilon}{\phi})\sigma_{all} \ \rightarrow \ \frac{\phi}{\phi+\varepsilon(1-\phi)}\sigma_{von} \le \sigma_{all} \\ &\Phi_{\min} \le \Phi_{i,j} \le 1 \quad i=1,...,n \ , \ j=1,...,m \end{aligned} \tag{14}$$

where σ_{all} and Φ_{min} are the allowable stress value and the lower bound of design variables, respectively. The expression that is multiplied by the von Mises stress level, is called relaxation coefficient wherein ε is considered as the small positive value [46]. Also, the function value of ϕ is calculated in the stress point of each constraint.

From Equations (9) and (11) the coefficient matrix **K** can be written as follows:

$$\mathbf{K}=\sum_{p=1}^{np}\mathbf{K}^p=\sum_{p=1}^{np}\int_{\Omega^p}\mathbf{B}^T\phi^{\mu}\mathbf{C}^0\mathbf{B}d\Omega \tag{15}$$

where *np* is the number of patches in the design domain which are assembled similar to the conventional finite element method.

4. SENSITIVITY ANALYSIS

In order to solve structural optimization problems by generating a sequence of explicit first order approximations, such as MMA [10], one needs to differentiate the objective function and all constraint functions with respect to the design variables. The procedure to obtain

these derivatives is called sensitivity analysis. There are two main groups of methods: numerical methods, and analytical methods. One may also consider hybrids of methods from these two groups: so-called semi-analytical methods. Also, there are two different analytical methods: the so-called direct and adjoint methods [1,47-49]. In this research, direct analytical method is utilized for calculating derivatives of the local stress constraints. Since relaxation coefficient depends on design variables, the chain rule needs to be used in order to differentiate the stress constraints. Therefore:

$$\frac{\partial \text{ stress constraint}}{\partial \Phi_{i,j}} = A' \times \sigma_{von} + A \times \frac{\partial \sigma_{von}}{\partial \Phi_{i,j}} \tag{16}$$

where A denotes the relaxation coefficient. Using Equation (13), derivatives of von Mises stresses with respect to the design variables, which are considered as the third component of the density surface control points' coordination, is calculated as below:

$$\frac{\partial \sigma_{von}}{\partial \Phi_{i,j}} = \frac{\frac{\partial}{\partial \Phi_{i,j}}(\sigma_x^2 + \sigma_y^2 - \sigma_x \sigma_y + 3\tau_{xy}^2)}{2\sigma_{von}} = \frac{\frac{\partial \sigma_x}{\partial \Phi_{i,j}}(2\sigma_x - \sigma_y) + \frac{\partial \sigma_y}{\partial \Phi_{i,j}}(2\sigma_y - \sigma_x) + 6\tau_{xy}\frac{\partial \tau_{xy}}{\partial \Phi_{i,j}}}{2\sigma_{von}} \tag{17}$$

Differentiating both sides of the constitutive equation (7) gives derivatives of the stress components as:

$$\frac{\partial \boldsymbol{\sigma}}{\partial \Phi_{i,j}} = \mathbf{C}\mathbf{B}\frac{\partial \mathbf{u}}{\partial \Phi_{i,j}} \tag{18}$$

Also, differentiating the equilibrium (**Ku=f**) obtains:

$$\mathbf{K}\frac{\partial \mathbf{u}}{\partial \Phi_{i,j}} + \frac{\partial \mathbf{K}}{\partial \Phi_{i,j}}\mathbf{u} = \frac{\partial \mathbf{f}}{\partial \Phi_{i,j}} \tag{19}$$

In the absence of body forces, the right-hand side of Equation (19) will be zero, therefore:

$$\mathbf{K}\frac{\partial \mathbf{u}}{\partial \Phi_{i,j}} = -\frac{\partial \mathbf{K}}{\partial \Phi_{i,j}}\mathbf{u} \tag{20}$$

Since Equation (20) has the same form as the equilibrium, the right-hand side of (20) is often called pseudo-load [1,47-49]. In order to obtain the pseudo-load vector, derivatives of global coefficient matrix **K** with respect to design variables can be derived as below:

$$\frac{\partial \mathbf{K}}{\partial \Phi_{i,j}} = \sum_{p=1}^{np} \int_{\Omega^p} \mathbf{B}^T (\mu \phi^{\mu-1} R(\xi,\eta)) \mathbf{C}^0 \mathbf{B} d\Omega \tag{21}$$

Substituting (21) into (20) and solving the obtained equation, derivatives of displacements with respect to the design variables are calculated and plugged into (18) to find derivatives of stress vector (18) and, eventually, the von Mises stress derivatives in (17).

For the sake of completeness in terms of stress constraints differentiation in (16), derivatives of the relaxation coefficient after some manipulations are obtained as follows:

$$A' = \frac{R(\xi,\eta)\varepsilon}{\varepsilon^2(1+\phi^2-2\phi)+2\phi\varepsilon+\phi^2(1-2\varepsilon)} \tag{22}$$

Finally, derivatives of the objective function, i.e. weight of structure in Equation (12), with respect to the design variables can be written as follows:

$$\frac{\partial W}{\partial \Phi_{i,j}} = \int_{\Omega} R(\xi,\eta)d\Omega \tag{23}$$

5. NUMERICAL EXAMPLES

In this section, three examples are presented to demonstrate performance and accuracy of the proposed algorithm as well as the sensitivity analysis in weight minimization problems under stress constraints.

5.1 Example 1

A short cantilever beam subjected to a point load at the bottom corner is considered, as shown in Figure 1. The beam has been modeled with one patch and 1066 control points. The modulus of elasticity and the poisson's ratio are considered as 1500 kgf/cm^2 and 0.3, respectively. Also, the exponent μ=3 penalizes the density function to prevent generating gray regions. Dimensions of the design domain are assumed as L=8 *cm* and H=5 *cm*. In addition, the point load magnitude is taken as P=100*kgf*. In all of the discretizations, equally spaced open knot vectors are used for each direction. The considered knot vectors are given in Table 1. The ε parameter and the allowable stress are considered to be 0.1 and 570 kgf/cm^2, respectively. Stress constraints of the problem are worked out in 625 uniformly distributed stress points.

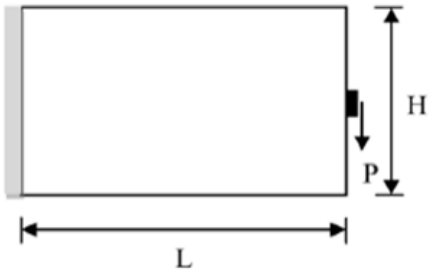

Figure 1. Short cantilever beam

Table 1: Considered knot vectors for each patch (Examples 1 & 2)

The employed equally spaced knot vectors	No. of Control Points
Ξ={0,0,0,0.025641,…,0.974358,1,1,1} for p=2	
H={0,0,0,0.041666,…,0.958318,1,1,1} for q=2	1066
Ξ={0,0,0,0.066,…,0.933,1,1,1} for p=2	187
H={0,0,0,0.111,…,0.889,1,1,1} for q=2	

The obtained topology is depicted in Figure 2(a). For the sake of comparison, the optimum layout using the level set method and the Finite Cell Method (FCM) from Reference [50] is shown in Figure 2(b). The design domain is partitioned into 80 × 50 cells. As it is shown the layouts are approximately the same, however, wiggly boundaries in the proposed topology are emerged due to the control points' distances. In other words, using more control points can lead to have more non-gray areas and smoother boundaries.

The stress contour plot is depicted in Figure 2(c) where the stresses have been kept less than the allowable stress by the algorithm. Also, the iteration history presented in Figure 2(d) expresses appropriate performance of MMA in optimization problems with high number of constraints.

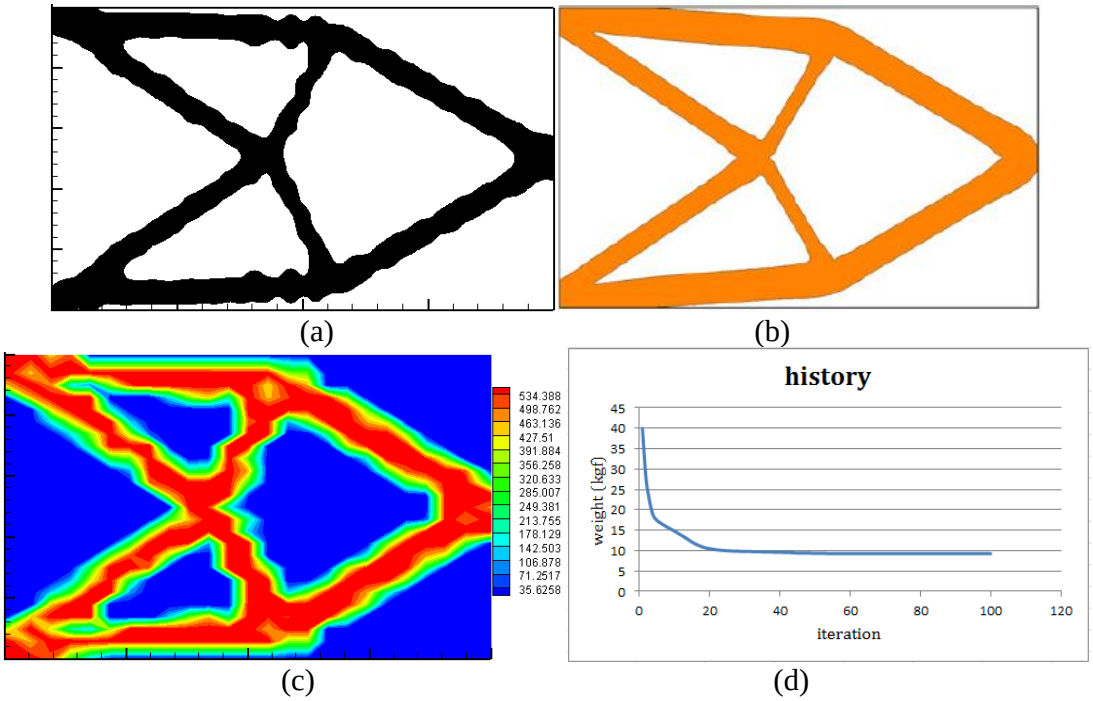

Figure 2. short cantilever beam: (a) optimum layout in present work; (b) optimum layout in Reference [50] with FCM/LS method; (c) stress contour plot; (d) iteration history for objective function

5.2 Example 2

In this example, the ability of the present work in capturing the optimum topology and the effect of number of control points and stress constraints is studied. For this purpose, a couple

of control nets with 187 and 1066 points are used for discretizing the design domain as well as the material density function. 121 and 625 stress points are uniformly considered for calculating the Von Mises stress constraints, respectively, for both assumed discretizations. The geometry, loading and boundary conditions are illustrated in Figure 3. The allowable stress is taken 1620 kgf/cm^2. All other parameters are assumed to be the same as previous example.

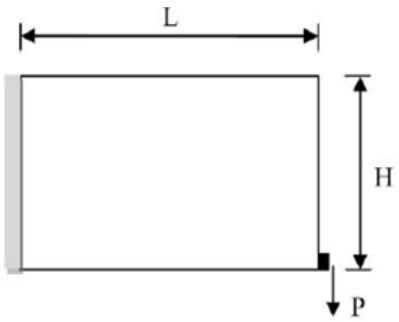

Figure 3.short cantilever beam

The optimum topologies are illustrated in Figures 4(a) and 4(b) for 187 and 1066 control points, respectively. Also, their corresponding stresses plot are depicted in Figures 4(c) and 4(d) for 121 and 625 stress constraints, respectively. As it is observed, by increasing the number of control points layouts with less intermediate material densities, i.e. gray areas, are obtained. According to the iteration histories (Figures 4(e) and 4(f)), the optimum weight of the structure is obtained 5.63 *kgf* and 4.80 *kgf* for 187 and 1066 control points, respectively. Results show that elimination of gray areas due to increase of the control points can lead to lighter structure.

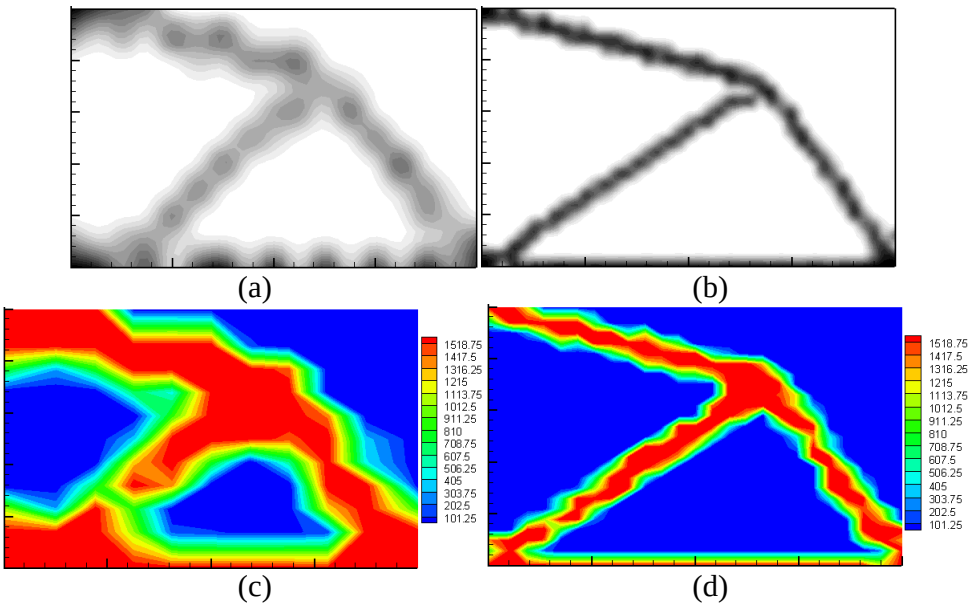

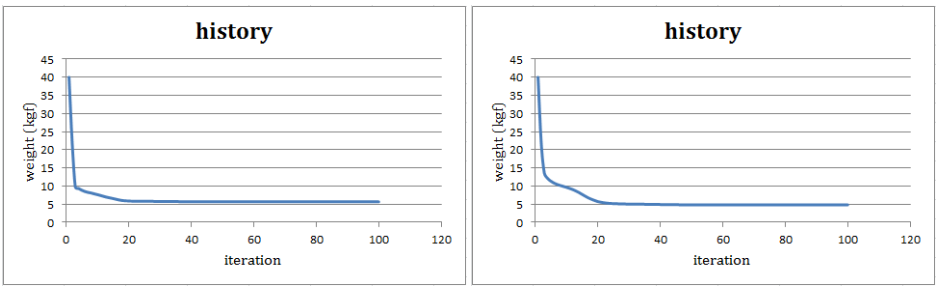

(e) (f)

Figure 4. short cantilever beam: (a), (b) optimum layouts; (c), (d) stress contour plots; (e), (f) iteration history for objective functions of using 187 and 1066 control points.

5.3 Example 3

An L-shaped structure is studied in this example. Figure 5 shows the geometry, loading and boundary conditions of the problem. Other parameters is considered as E=100 *Pa*; v=0.3; L=1.0 *m*; P=1.0 *N*; μ=3; ε=0.1. The design domain is created by using 3 patches and 1701 control points. The used open knot vectors are given in Table 2. Stress constraints are calculated in 324 uniformly distributed stress points in each patch and the stress limitation is considered to be 100 kgf/cm^2.

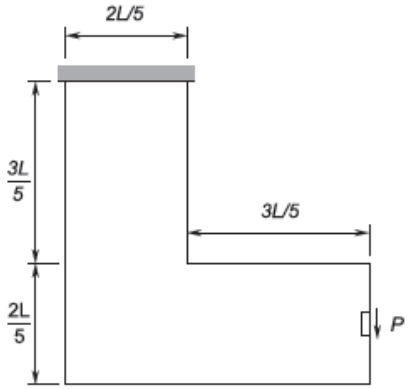

Figure 5. L-shaped structure

Table 2: Considered knot vectors for each patch

The employed equally spaced knot vectors	No. of Control Points
Ξ=H={0,0,0,0.052631,…,0.947358,1,1,1},p=q=2	1
Ξ={0,0,0,0.052631,…,0.947358,1,1,1} for p=2 H={0,0,0,0.034482,…,0.965496,1,1,1} for q=2	2
Ξ={0,0,0,0.034482,…,0.965496,1,1,1} for p=2 H={0,0,0,0.052631,…,0.947358,1,1,1} for q=2	3

Figures 6(a) and 6(c) demonstrate the obtained topology and stress contour plot considering weight minimization under stress constraints. The iteration history is depicted in Figure 6(d). The minimum weight is obtained 0.128 *kgf* that is %20 of the initial weight of

the structure which is 0.64 *kgf*.

On the other hand, the topology optimization has been carried out considering minimization of the mean compliance with a certain amount of materials which gives the stiffest possible structure. For the sake of comparison, the volume fraction is considered to be 20%. The final topology is shown in Figure 6(b). It is observed that the weight minimization approach subject to local stress constraints leads to a more rounded boundary on the corner and avoid stress concentration.

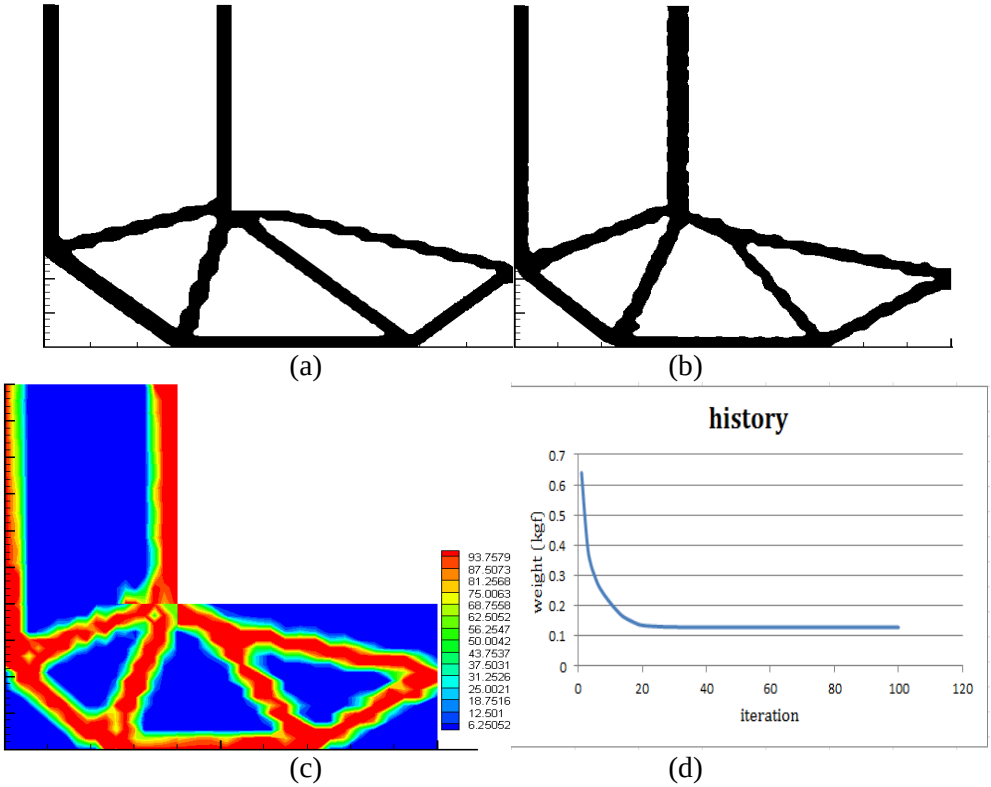

Figure 6. L-shaped structure: (a) optimum topology for weight minimization formulation; (b) optimum topology for traditional formulation; (c) stress contour plot (d) iteration history for objective function

6. CONCLUSION

In this research, the IA method is utilized for structural topology optimization considering weight minimization under local stress constraints. The sensitivity analysis is carried out based on the direct differentiation and the outcomes are used in the gradient-based MMA algorithm. The stress relaxation technique is also used in definition of the optimization problem in order to avoid the singularity problem. Performance of the employed algorithm and the direct sensitivity analysis is shown through the numerical examples. The results are compared with outcomes from other methods of topology optimization and show similar topologies. Increasing number of control points leads to elimination of gray areas as well as

smoother boundaries. Furthermore, selection of an appropriate relaxation parameter causes all the constraints to be satisfied. In the third numerical example, comparing the minimum weight formulation with the common mean compliance approach, different optimum layouts are obtained and more reasonable layout without stress concentration is formed when minimum weight formulation is employed.

Acknowledgement: The Authors would like to thank Professor Krister Svanberg for providing the MMA code.

REFERENCES

1. Christensen PW, Klarbring A. *An Introduction to Structural Optimization*, Springer, Sweden, 2009.
2. Bendsøe MP, Sigmund O. *Topology Optimization; Theory, Methods and Applications*, Springer, Germany, 2003.
3. Bendsøe MP, Kikuchi N. Generating optimal topologies in structural design using a homogenization method, *Comput Method Appl Mech* 1988; **71**: 197-224.
4. Rozvany GIN. *Structural Design via Optimality Criteria*, Kluwer Academic Publishers, Dordrecht, 1989.
5. Rozvany GIN, Zhou M. The COC algorithm, Part I: Cross section optimization or sizing, *Comp Meth Appl Mech Eng* 1991; **89**: 281-308.
6. Schmit LA, Farsi B. Some approximation concepts for structural synthesis, *AIAA J* 1974; **12**(5): 692-9.
7. Schmit LA, Miura H. *Approximation Concepts for Efficient Structural Synthesis*, NASA CR-2552, 1976.
8. Vanderplaats GN, Salajegheh E. A new approximation method for stress constraints in structural synthesis, *AIAA J* 1989; **27**(3): 352-8.
9. Fleury C. CONLIN: An efficient dual optimizer based on convex approximation concepts, *Struct Multidisc Optim* 1989; **1**: 81-9.
10. Svanberg K. The method of moving asymptotes – a new method for structural optimization, *Int J Numer Meth Eng* 1987; **24**: 359-73.
11. Kane C, Schoenauer M. Topological optimum design using genetic algorithms, Special Issue on Optimum Design, *Contr Cybern* 1996; **25**(5): 1059-88.
12. Fanjoy D, Crossley W. Using a genetic algorithm to design beam corss-sectional topology for bending, torsion, and combined loading, *Structural Dynamics and Material Conference and Exhibit*, AIAA, Atlanta, GA, 2000, pp. 1-9.
13. Jakiela MJ, Chapman C, Duda J, Adewuya A, Saitou K. Continuum structural topology design with genetic algorithms, *Comput Meth Appl Mech Eng* 2000; **186**: 339-56.
14. Kaveh A, Hassani B, Shojaee S, Tavakkoli SM. Structural topology optimization using ant colony methodology. *Eng Struct* 2008; **30**(9): 2559-65.
15. Xie YM, Steven GP. A simple evolutionary procedure for structural optimization, *Comput Struct* 1993; **49**(5): 885-96.
16. Sethian J, Wiegmann A. Structural boundary design via level set and immersed interface methods, *J Comput Phys* 2000; **163**: 489-528.

17. Wang MY, Wang X, Guo D. A level-set method for structural topology optimization, *Comput Meth Appl Mech Eng* 2003; **192**: 227-46.
18. Allaire G, Jouve F, Toader AM. Structural optimization using sensitivity analysis and a level-set method, *J Comput Phys* 2004; **194**:363 -93.
19. Belytschko T, Xiao SP, Parimi C. Topology optimization with implicit functions and regularization, *Int J Numer Meth Eng* 2003; **57**: 1177-96.
20. Duysinx P, Bendsøe MP. Topology optimization of continuum structures with local stress constraints, *Int J Numer Meth Eng* 1988; **43**: 1453-78.
21. Duysinx P, Sigmund O. New developments in handling stress constraints in optimal material distributions, *7th Symposium on Multidisciplinary Analysis and Optimization*, AIAA/USAF/ NASA/ISSMO, 1998, pp. 1501-9.
22. Duysinx P. Topology optimization with different stress limits in tension and compression, *Third World Congress of Structural and Multidisciplinary Optimization*, University of New York at Buffalo, 2000.
23. Paris J, Navarrina F, Colominas I, Casteleiro M. Topology optimization of continuum structures with local and global stress constraints, *Struct Multidisc Optim* 2009; **39**: 419-37.
24. Paris J, Navarrina F, Colominas I, Casteleiro M. Block aggregation of stress constraints in topology optimization of structures, *Adv Eng Softw* 2010; **41**: 433-41.
25. Le C, Norato J, Bruns T, Ha C, Tortorelli D. Stress-based topology optimization for continua, *Struct Multidisc Optim* 2010; **41**: 605-20.
26. Holmberg E, Torstenfelt B, Klarbring A. Stress constrained topology optimization, *Struct Multidisc Optim* 2013; **48**: 33-47.
27. Paris J, Colominas I, Navarrina F, Casteleiro M. Parallel computing in topology optimization of structures with stress constraints, *Computers and Structures* 2013; **125**: 62-73.
28. Luo Y, Wang MY, Kang Z. An enhanced aggregation method for topology optimization with local stress constraints, *Comput Meth Appl Mech Eng* 2013; **254**: 31-41.
29. Huan-Huan G, Ji-Hong Z, Wei-Hong Z, Ying Z. An improved adaptive constraint aggregation for integrated layout and topology optimization, *Comput Meth Appl Mech Eng* 2015; **289**: 387-408.
30. Kennedy GJ. Strategies for adaptive optimization with aggregation constraints using interior-point methods, *Comput Struct* 2015; **153**: 217-29.
31. Paris J, Navarrina F, Colominas I, Casteleiro M. Improvements in the treatment of stress constraints in structural topology optimization problems, *J Comput Appl Math* 2010; **234**: 2231-8.
32. Sved G, Ginos Z. Structural optimization under multiple loading, *Int J Mech Sci* 1968; **10**: 803-5.
33. Kirsch U. On singular topologies in optimum structural design, *Struct Multidisc Optim* 1990; **2**: 133-42.
34. Rozvany G, Birker T. On singular topologies in exact layout optimization, *Struct Multidisc Optim* 1994; **8**: 228-35.
35. Guo X, Cheng G, Yamazaki K. A new approach for the solution of singular optima in truss topology optimization with stress and local buckling constraints, *Struct Multidisc Optim* 2001; **22**: 364-73.

36. Cheng G, Guo X. ε-relaxed approach in structural topology optimization, *Struct Multidisc Optim* 1997; **13**: 258-66.
37. Hughes TJR, Cottrell JA, Bazilevs Y. Isogeometric analysis: CAD, finite elements, NURBS, exact geometry and mesh refinement, *Comput Meth Appl Mech Eng* 2005; **194**: 4135-95.
38. Bazilevs Y, Beirao Da Veiga L, Cottrell JA, Hughes TJR, Sangalli G. Isogeometric analysis: approximation, stability and error estimates for h-refined meshes, *Math Mod Meth Appl Sci* 2006; **16**: 1031-90.
39. Bazilevs Y, Calo VM, Cottrell J, Hughes TJR, Reali A, Scovazzi G. Variationalmultiscale residual-based turbulence modeling for large eddy simulation of incompressible flows, *Comput Meth Appl Mech Eng* 2007; **197**: 173-201.
40. Bazilevs Y, Calo VM, Zhang Y, Hughes TJR. Isogeometric fluid structure interaction analysis with applications to arterial blood flow, *Comput Meth Appl Mech Eng* 2006; **38**: 310-22.
41. Cottrell JA, Reali A, Bazilevs Y, Hughes TJR. Isogeometric analysis of structural vibrations, *Comput Meth Appl Mech Eng* 2006; **195**: 5257-96.
42. Hassani B, Khanzadi M, Tavakkoli SM. An isogeometrical approach to structural topology optimization by optimality criteria, *Struct Multidisc Optim* 2012; **45**: 223-33.
43. Tavakkoli SM, Hassani B, Ghasemnejad H. Isogeometric topology optimization of structures by using MMA, *Int J Optim Civ Eng* 2013; **3**: 313-26.
44. Piegl L, Tiller W. *The NURBS Book*, Springer, 2nd edition, Germany, 1995.
45. Hassani B, Hinton E. *Homogenization and Structural Topology Optimization: Theory, Practice and Software*, Springer, London, 1999.
46. Pereira JT, Fancello EA, Barcellos CS. Topology optimization of continuum structures with material failure constraints, *Struct Multidisc Optim* 2004; **26**: 50-66.
47. Haftka RT, Gurdal Z. *Elements of Structural Optimization*, Kluwer, 3rd revised and expanded edition, Dordrecht, 1992.
48. Choi KK, Kim NH. *Structural Sensitivity Analysis and Optimization 1—Linear Systems*, Springer, Berlin, 2005.
49. Choi KK, Kim NH. *Structural Sensitivity Analysis and Optimization 2—Nonlinear Systems and Applications*, Springer, Berlin, 2005.
50. Cai S, Zhang W. Stress constrained topology optimization with free-form design domains, *Comput Meth Appl Mech Eng* 2015; **289**: 267-90.